Learning-Based Modeling of Soft Actuators Using Euler Spiral-Inspired Curvature

Yu Mei, Shangyuan Yuan, Xinda Qi, Preston Fairchild and Xiaobo Tan

Department of Electrical and Computer Engineering
Michigan State University

Oct 06, 2025

MECC 2025

Background of Soft Robots

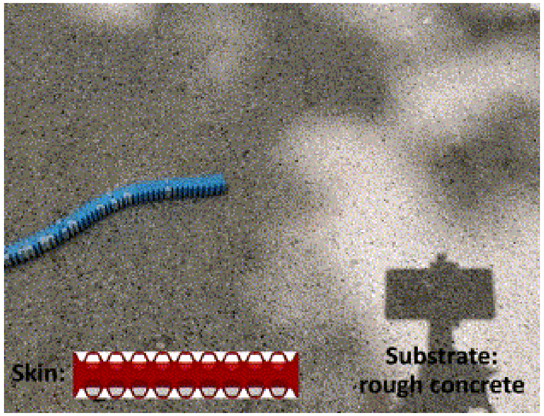

Figure: Soft snake robot [1]

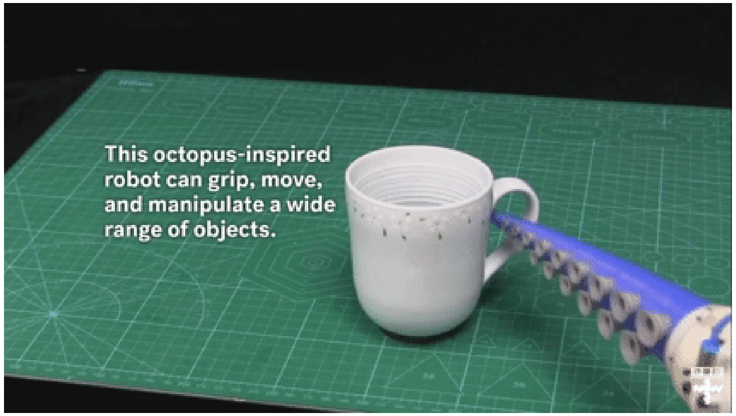

Figure: Octopus-inspired gripper [2]

Challenges

- ❑ Infinite degrees of freedom
- ❑ Actuation physics
- ❑ Environmental interaction

Categories of Modeling

- ❑ Piecewise constant curvature approach (PCC)
- ❑ Variable curvature approach (VC)

[1] Qi et al., Soft Robotics '18
[2] Xie et al., Soft Robotics '20

Piecewise Constant Curvature approach (PCC)

- PCC examples

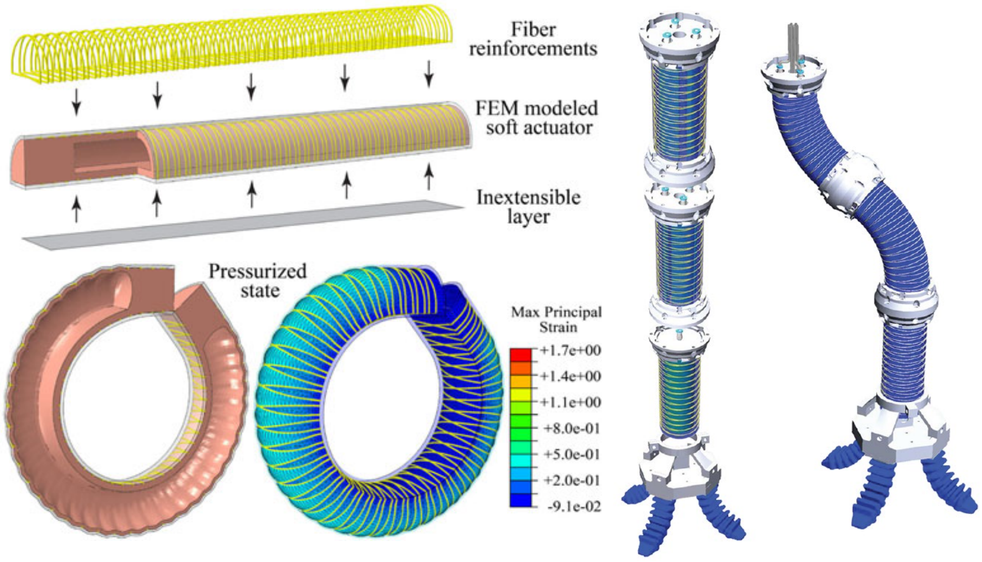

Figure: Soft bending actuators [3] and 3D soft manipulators [4]

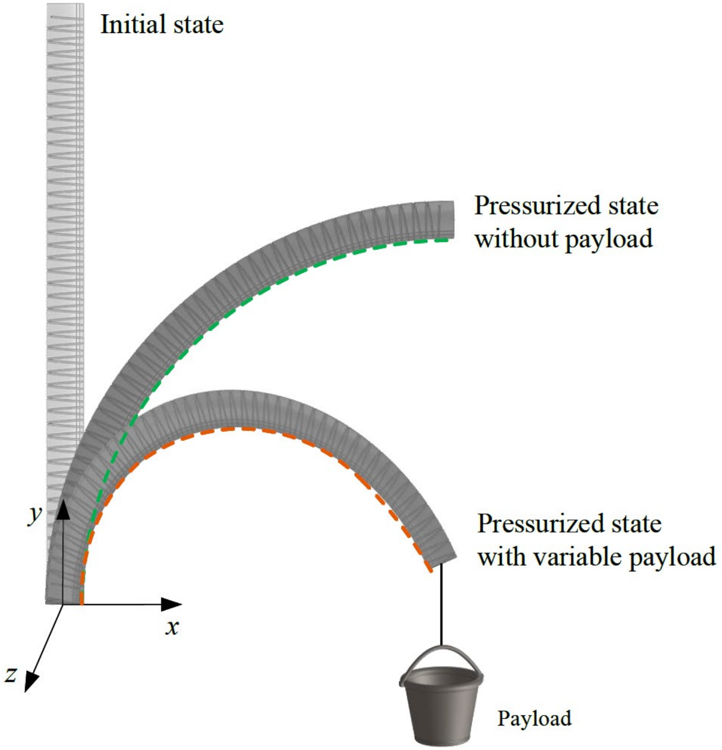

Limitation

It fails to capture the shape under relatively large payloads or gravity.

[3] Polygerinos et al., TRO '18
[4] Gong et al., IJRR '20

Variable Curvature approach (VC)

VC approaches

- Cosserat rod theory [Renda, TRO '18]
- Finite element method (FEM) [Wu, RAL '22]

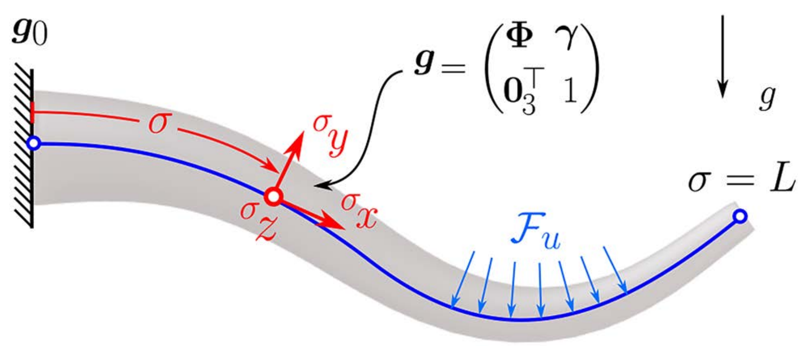

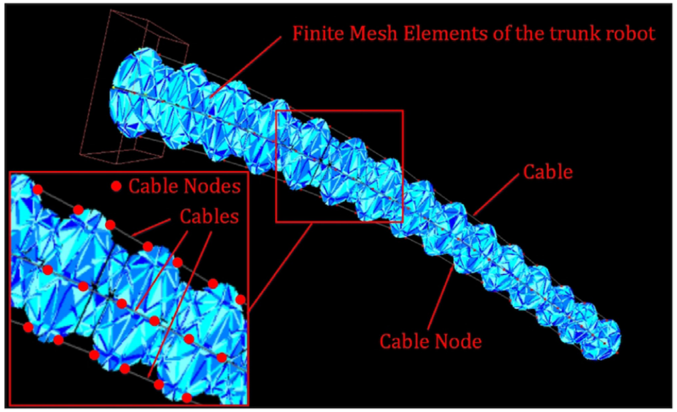

Limitation: High computational cost due to PDEs or large sets of coupled ODEs

Goal

Compact VC representation but still captures continuous shape with high-fidelity.

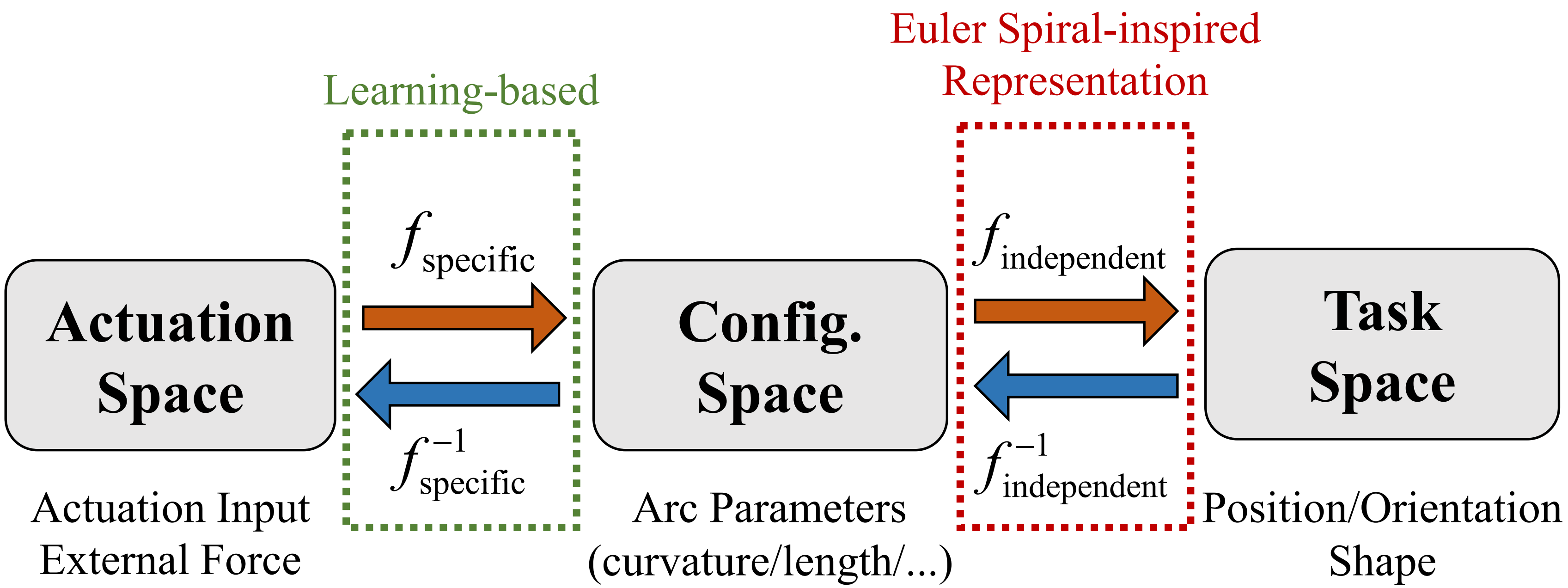

Figure: General framework of modeling for soft robots [5]

[5] Webster et al., IJRR '10

Euler Spiral

Definition

- Proposed in 1694 by Bernoulli as the classic elastica problem.
- The curvature changes linearly with respective to the arc length.

Applications

- Rail track transition design [6]
- Shape completion [7]

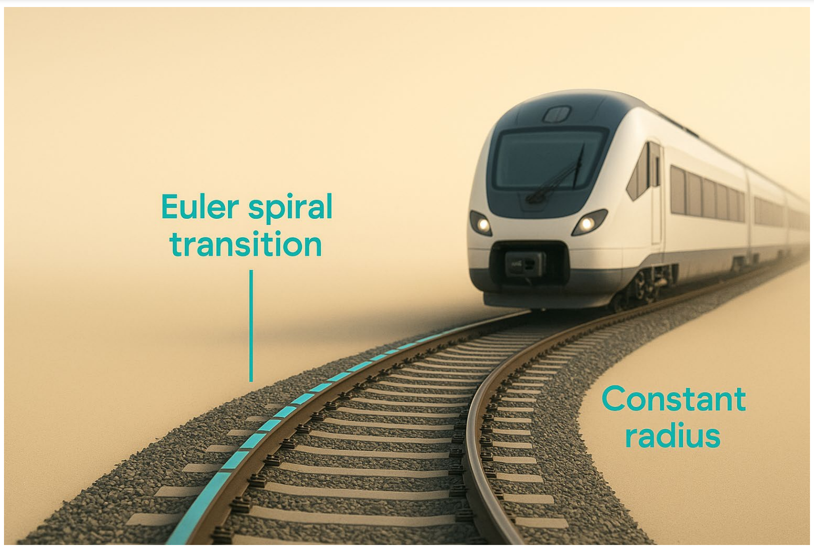

[6] Eliou et al., Eur. Transp. Res. Rev. '14;
[7] He et al., Vis. Comput. Ind. Biomed. Art. '21.

Shape Representation inspired by Euler Spiral

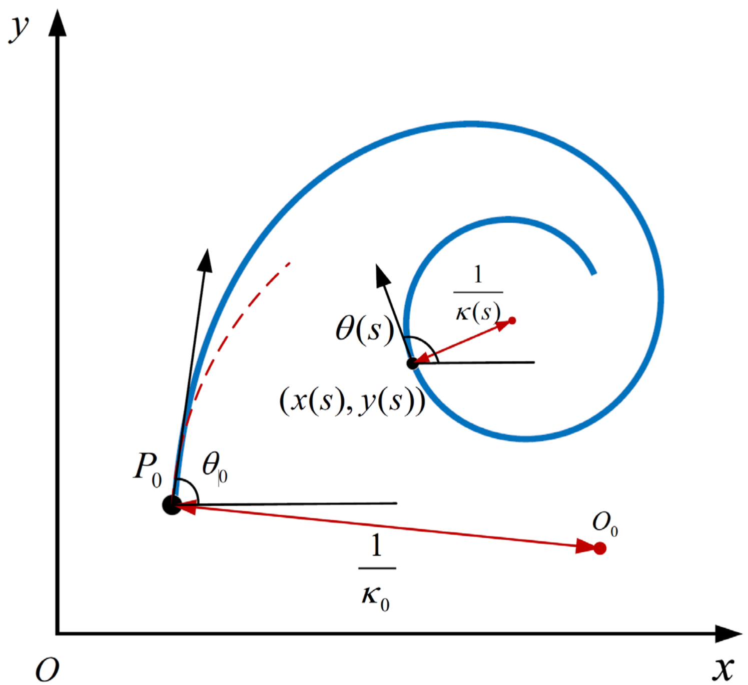

Figure: Illustration of the Euler Spiral

$$\begin{cases} \dot{x}(s) = \cos\theta(s), & x(0) = x_0, \\ \dot{y}(s) = \sin\theta(s), & y(0) = y_0, \\ \dot{\theta}(s) = \kappa(s), & \theta(0) = \theta_0, \end{cases} \quad (1)$$

Traditional: $\kappa(s) = \kappa_1 s + \kappa_0,$

Extended: $\kappa(s) = \sum_{k=0}^{N} \kappa_k s^k, \quad (2)$

By plugging Eq. (2) into Eq. (1), one can get:

$$\begin{cases} x(s) = \int_0^s \cos(\theta(\tau))d\tau + x_0, \\ y(s) = \int_0^s \sin(\theta(\tau))d\tau + y_0, \\ \theta(s) = \sum_{k=0}^{N} \frac{\kappa_k}{k+1} s^{k+1} + \theta_0, \end{cases} \quad (3)$$

The curve is compactly characterized by the shape parameters $\mathbf{q} = \{\kappa_k\} = [\kappa_0, \kappa_1, \ldots, \kappa_N]^T$.

Numerical Validation

- High-fidelity physical simulation for soft bending actuator (ground truth) [7]
- Validation Results (curve fitting)

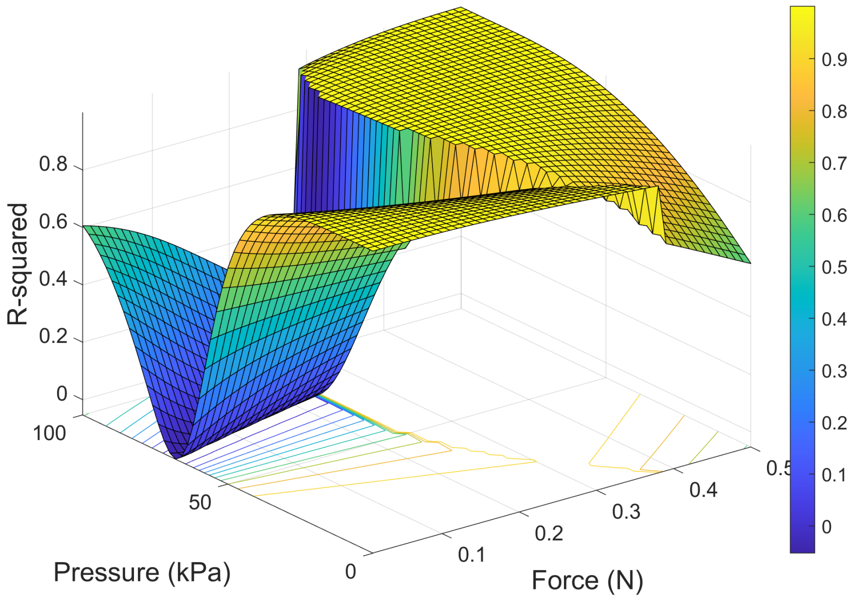

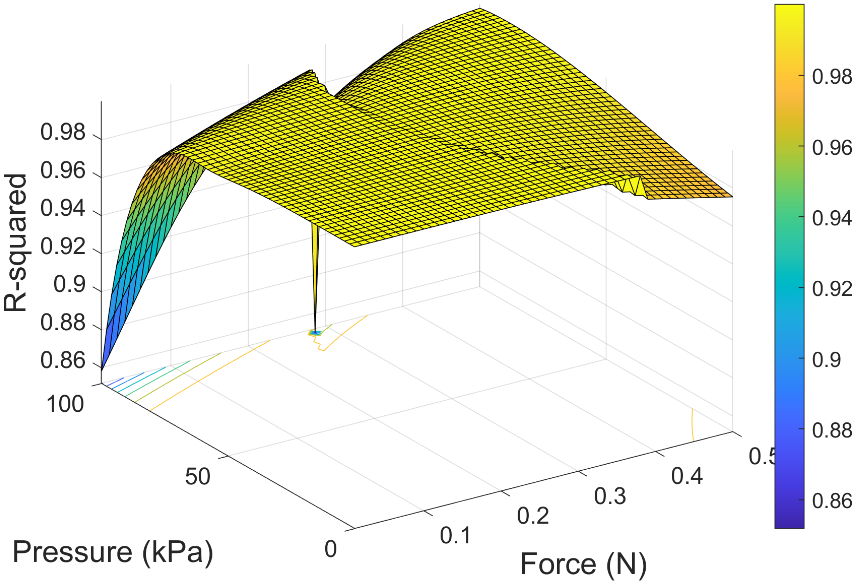

Traditional Euler Spiral with first order:

$$R^2 = 0.77 \pm 0.31$$

Quadratic Euler Spiral with second order:

$$R^2 = 0.99 \pm 0.01$$

[7] Mei et al., TMech '24

Learning-based Forward and Inverse Models

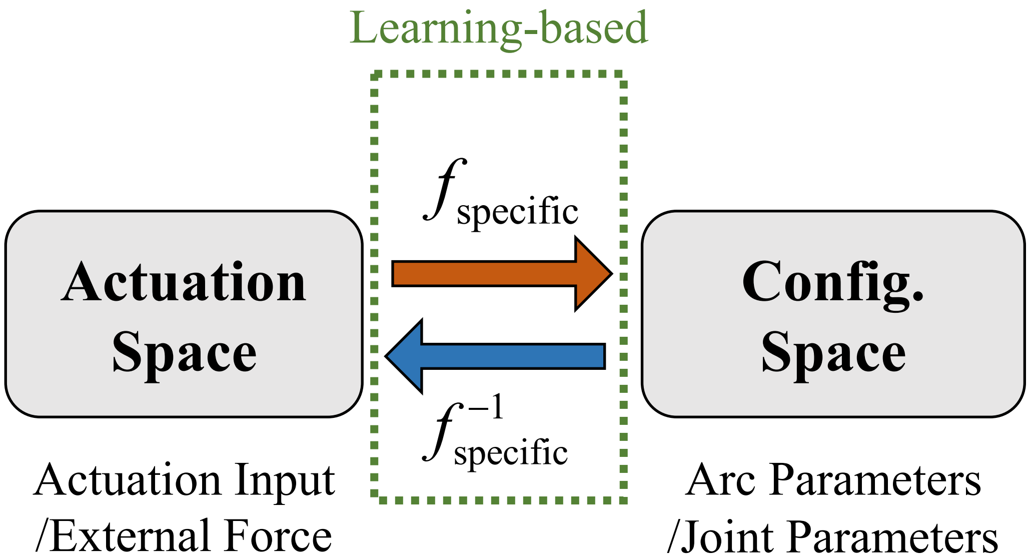

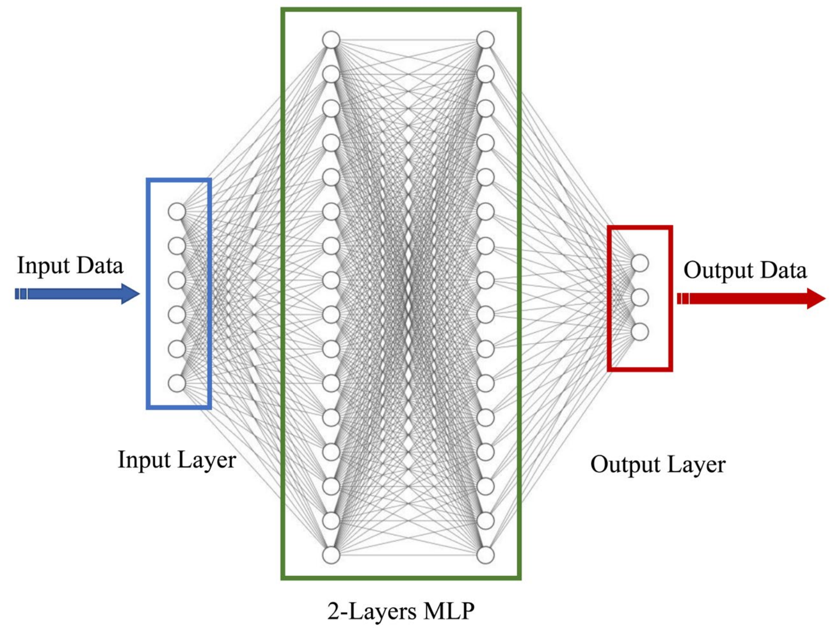

- Actuation input for this specific robot: Pneumatic input P, Payload W.
- Forward neural network: Input is $[P, W]^T$ and output is $\mathbf{q} = \boldsymbol{\kappa}^T$.
- Inverse neural network: Input is $[\mathbf{q}, P]^T$ and output is W.

Dataset collection: $[P, W, \mathbf{q}]$

Curvature Parameters Extraction

Challenge of Dataset Collection

The direct and accurate measurement of the curvature is not readily available.

G^1 Hermite Interpolation Problem

Finding a G^1 smooth curve fitting two given points P_0, P_1 and the corresponding orientation angles θ_0, θ_1.

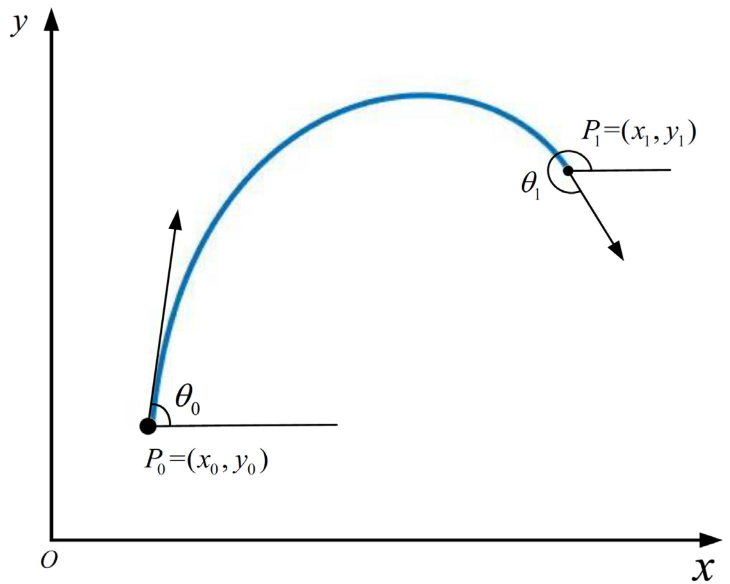

Figure: Illustration of G1 Hermite Interpolation

Optimization Problem:

$$\boldsymbol{\kappa}^* = \arg\min_{\boldsymbol{\kappa}\in\mathbb{R}^{N+1}} \left\| \begin{bmatrix} x(L;\boldsymbol{\kappa}) - x_1 \\ y(L;\boldsymbol{\kappa}) - y_1 \\ \theta(L;\boldsymbol{\kappa}) - \theta_1 \end{bmatrix} \right\|_2^2$$

$$\text{s.t.} \quad x(0) = x_0, \quad y(0) = y_0, \\ \dot{x}(0) = \cos\theta_0, \quad \dot{y}(0) = \sin\theta_0,$$

Experimental Setup

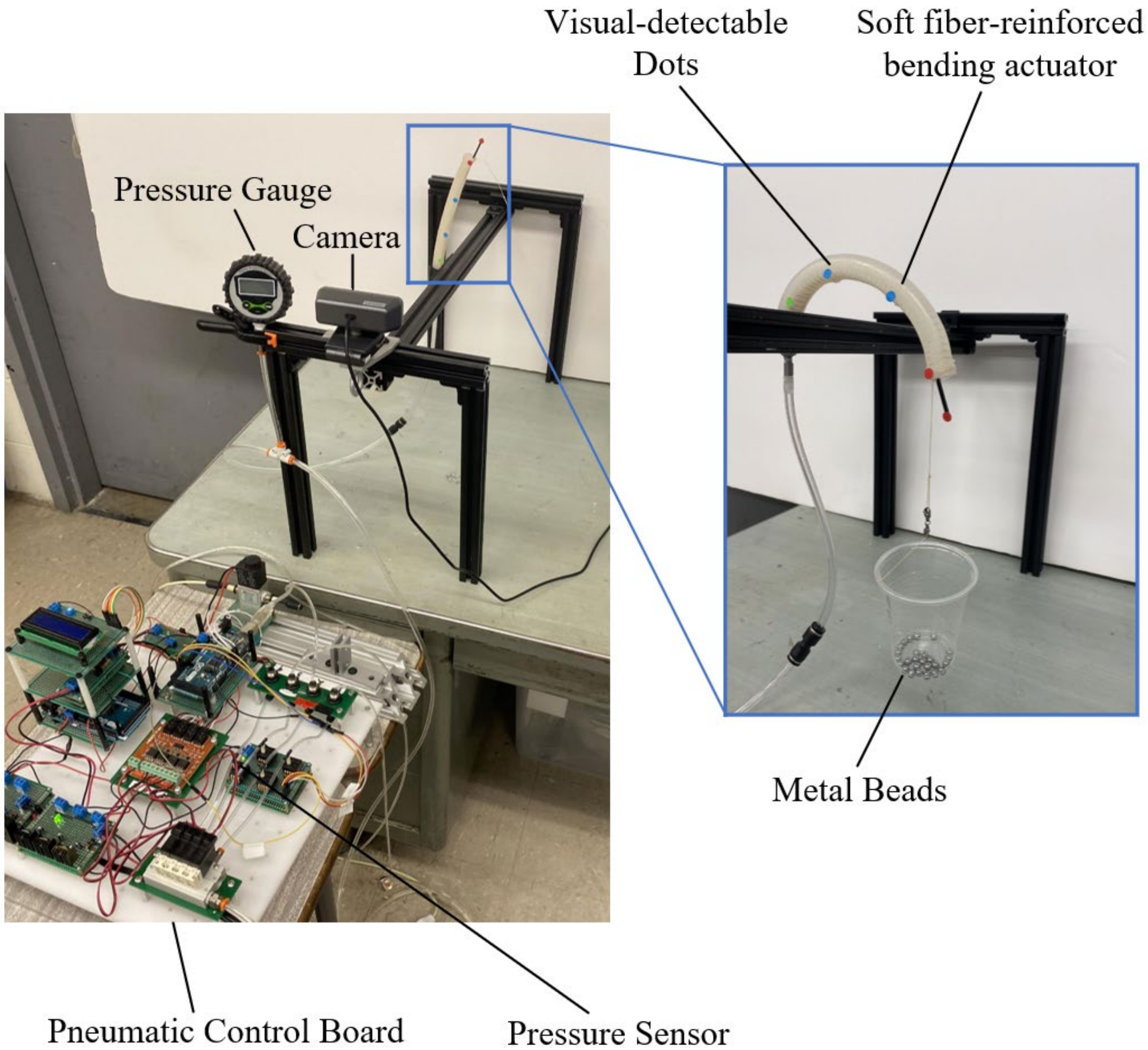

Model Prediction Results

❑ Forward Model Prediction Results

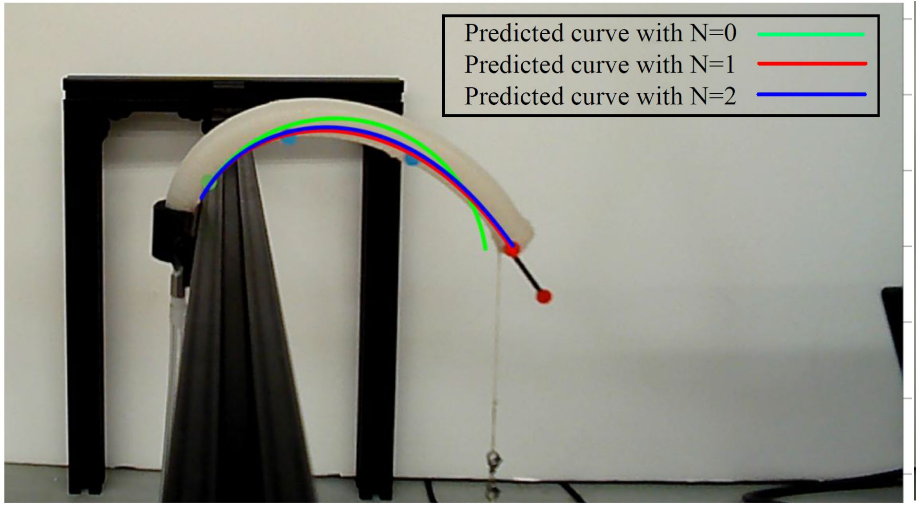

(a)

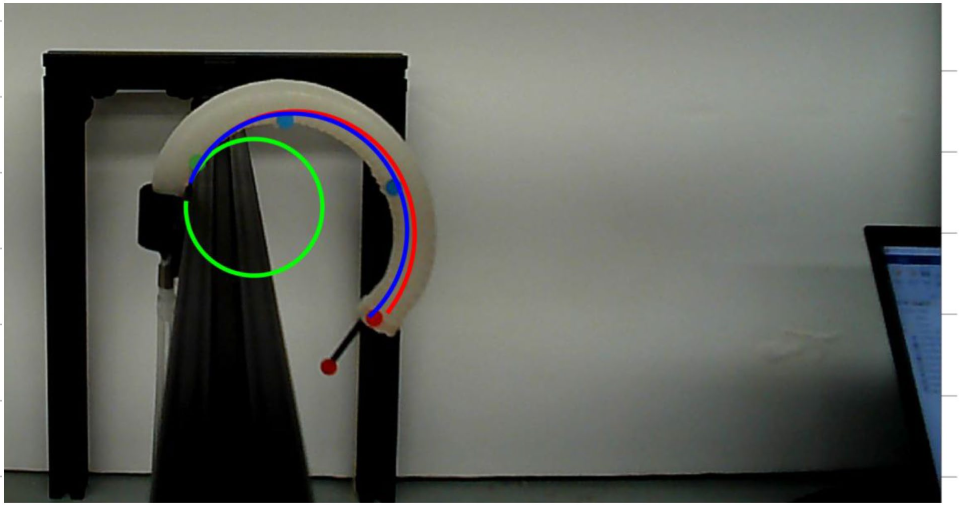

(b)

Table I. Average errors (%) at three reference points relative to actuator length.

	1/3 position error (%)	2/3 position error (%)	Tip error (%)
N=2	3.38 ± 0.21	2.19 ± 0.40	1.93 ± 1.33
N=1	3.43 ± 0.18	2.50 ± 0.45	2.02 ± 1.58
N=0	6.67 ± 4.24	17.5 ± 19.0	35.0 ± 35.0

Model Prediction Results

- Inverse Model Prediction Results

Table II. Average tipload errors (%) with respect to the range of the payload for different orders.

Order	Load Error (%)
N = 2	0.72 ± 0.62
N = 1	1.08 ± 1.12
N = 0	1.21 ± 1.08

Payload resolution is 0.254g for each bead (1%)

Conclusions

1. A compact VC representation but captures continuous shape with high-fidelity
2. Effective curvature extraction using G^1 Hermite interpolation
3. Learning-based model for robot-specific mapping
4. Experimental validations on actual robot

Future Work

1. Control-oriented dynamic model
2. Extend to 3D space with torsion

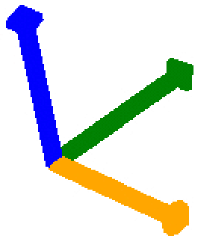

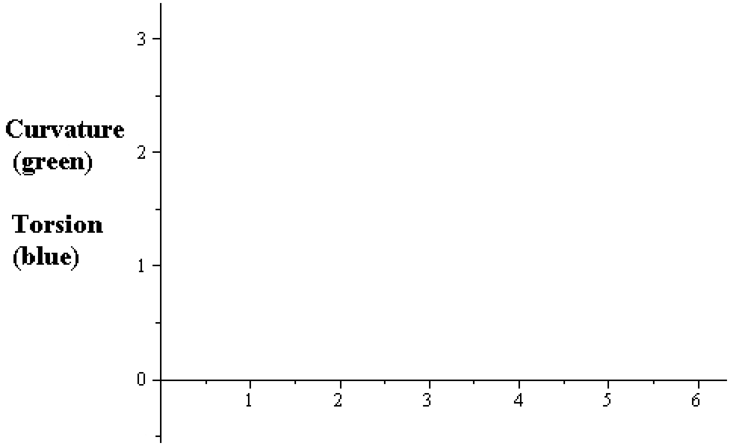

Acknowledgements:

This research was supported in part by National Science Foundation awards (CNS 2237577, ECCS 2024649 and CMMI 1940950).

Thank you!

Reference

1. X. Qi, T. Gao, and X. Tan, "Bioinspired 3D-Printed Snakeskins Enable Effective Serpentine Locomotion of a Soft Robotic Snake," *Soft Robotics*, p. soro.2022.0051, Nov. 2022.
2. Z. Xie, W. Li *et al.*, "Octopus Arm-Inspired Tapered Soft Actuators with Suckers for Improved Grasping," *Soft Robotics*, vol. 7, no. 5, pp. 639–648, Oct. 2020.
3. P. Polygerinos *et al.*, "Modeling of Soft Fiber-Reinforced Bending Actuators," *IEEE Transactions on Robotics*, vol. 31, no. 3, pp. 778–789, Jun. 2015.
4. Z. Gong *et al.*, "A soft manipulator for efficient delicate grasping in shallow water: Modeling, control, and real-world experiments," *The International Journal of Robotics Research*, vol. 40, no. 1, pp. 449–469, Jan. 2021.
5. B. Caasenbrood, A. Pogromsky, and H. Nijmeijer, "Energy-Shaping Controllers for Soft Robot Manipulators Through Port-Hamiltonian Cosserat Models," *SN COMPUT. SCI.*, vol. 3, no. 6, p. 494, Sep. 2022.
6. K. Wu, G. Zheng, and J. Zhang, "FEM-based trajectory tracking control of a soft trunk robot," *Robotics and Autonomous Systems*, vol. 150, p. 103961, Apr. 2022.
7. S. Sadati *et al.*, "Reduced Order vs. Discretized Lumped System Models with Absolute and Relative States for Continuum Manipulators," in *Robotics: Science and Systems XV*, Robotics: Science and Systems Foundation, Jun. 2019.
8. R. J. Webster and B. A. Jones, "Design and Kinematic Modeling of Constant Curvature Continuum Robots: A Review," *The International Journal of Robotics Research*, vol. 29, no. 13, pp. 1661–1683, Nov. 2010.
9. R. Levien, "The Euler spiral: a mathematical history", 2008.
10. N. Eliou and G. Kaliabetsos, "A new, simple and accurate transition curve type, for use in road and railway alignment design," Eur. Transp. Res. Rev., vol. 6, no. 2, pp. 171–179, Jun. 2014.
11. C. He, G. Zhao, A. Wang, F. Hou, Z. Cai, and S. Li, "Typical curve with G1 constraints for curve completion," Vis. Comput. Ind. Biomed. Art, vol. 4, no. 1, p. 28, Dec. 2021.
12. P. Rao, Q. Peyron, and J. Burgner-Kahrs, "Using Euler Curves to Model Continuum Robots," in 2021 IEEE International Conference on Robotics and Automation (ICRA), May 2021, pp. 1402–1408.
13. Y. Mei *et al.*, "Simultaneous Shape Reconstruction and Force Estimation of Soft Bending Actuators Using Distributed Inductive Curvature Sensors," *IEEE/ASME Trans. Mechatron.*, pp. 1–9, 2024.